Development and Application of a Wave Energy Conversion Simulation Model

J. Fairhurst[#1], J. L. van Niekerk[#2]

[#]*Centre for Renewable and Sustainable Energy Studies,*
Stellenbosch University
Stellenbosch Central, 7599, South Africa

[1]jasonfairhurst@sun.ac.za

[2]wikus@sun.ac.za

Abstract— **Abstract— This paper presents the development and application of a time-domain simulation model for a series of submerged, oscillating water columns. The original device was developed and patented by Stellenbosch University as the Stellenbosch Wave Energy Converter (SWEC). The main objective of this research was to develop a verified and validated simulation model for the SWEC and then to apply this model to full-scale sea conditions. A scale-model of a single chamber was experimentally tested and modelled; the resulting simulation model provides a better understanding of the hydrodynamic and thermodynamic behaviour of the chambers and the ability of the device to convert wave power into usable mechanical power. The model proved to be relatively accurate when predicting the power conversion with an overall average error of 12%. In addition, this paper also presents the simulation results for the expected wave power conversion for a site off the south coast of South Africa, near East London. The simulations used recorded wave data as input and predicted an average annual production of 4 289 MWh per SWEC plant with a calculated capacity factor of 35%.**

***Keywords*— Wave energy, hydrodynamics, thermodynamics, OWC, experimental, modelling.**

I. Introduction

The world is currently (2017) experiencing a global shift to clean, renewable energy. South Africa is an example of a country heavily dependent on fossil fuels to satisfy the energy needs over many years. These fuels are a finite resource and the energy extraction process is harmful to the environment, mainly because of the CO_2 emissions. Thus, there is an urgent need for power from alternative, reliable and sustainable energy sources. Wave energy has the potential to be a contributor to a sustainable solution of South Africa's energy needs.

The south-east coast of South Africa is roughly 700 km long with an average wave power of 25 kW/m [1]. If this energy could be harnessed efficiently it could provide support to South Africa's electrical grid. Many different WEC (Wave Energy Converter) concepts and designs exist throughout the world although very few have been implemented and connected to the grid on a commercial basis. This is due to challenges which exist in three aspects; survivability in a hostile environment, conversion efficiency and capital cost. In order for a WEC to be implemented it must prove to have sufficiently high energy-conversion efficiency as well as the ability to survive in the harsh ocean environment. As mentioned, this project focussed on accurately modelling the SWEC design that will aid in establishing the viability of the device in actual wave conditions, the simulation model is based on the work carried out by [2] and [3].

The SWEC is made up of two 160m long submerged arms, these arms are made up of OWCs (Oscillating Water Columns) and are positioned in a 'V' shape fixed to the sea floor. The arms consists of a number of units, these units each have three chambers that act as submerged OWC's. The turbine generator unit is fixed to a tower above the waterline at the apex of the 'V', see Fig. 1.

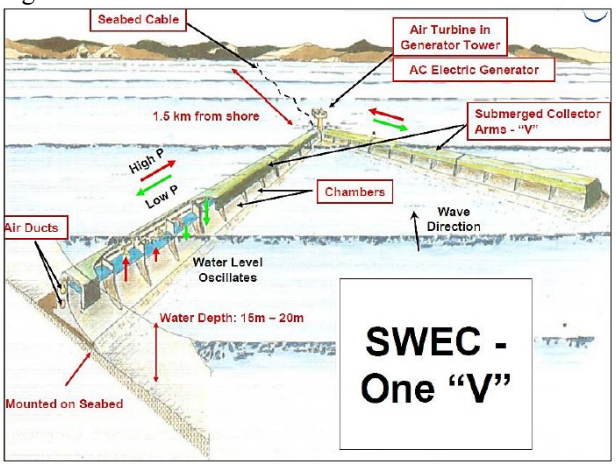

Fig. 1 Artist's rendition of the SWEC [4].

The SWEC was designed to operate off the south west coast of South Africa in wave conditions indicated in Table I [4]. As the crest of a wave moves overhead, water is forced into the submerged OWC's. Each OWC is connected to a high-pressure duct and a low-pressure duct by means of one-way valves. As water is forced into an OWC, the chamber pressure increases and forces air into the 'high pressure duct'. As the trough of a wave passes overhead the pressure decreases again and air is sucked out of the 'low pressure duct', see Fig. 2. This results in the low-pressure duct always being at a lower pressure than the high-pressure duct. The constant pressure differential between the two ducts induces an airflow that drives a turbine-generator unit on the top of the tower at the apex. The SWEC

has been designed to absorb only a portion (typically 30% [5]) of the wave energy passing overhead in order not to disrupt the natural motion of the waves and the sediment transportation that occurs in the deployment area.

TABLE II
PROPOSED OPERATING CONDITIONS FOR THE SWEC [4]

Wave parameter	Value	Unit
Wave height	2	m
Water depth	15-20	m
Wave period	12.3	s
Wave length	148.6	m

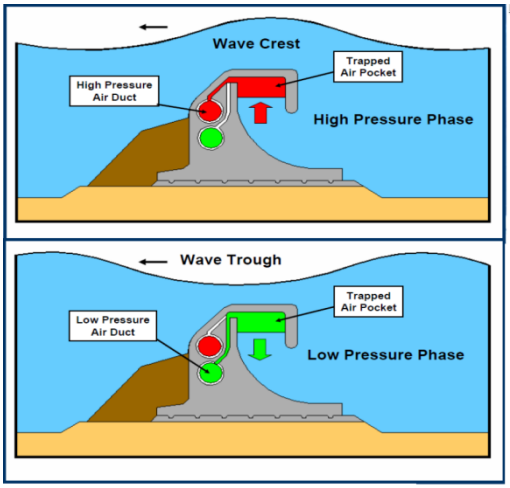

Fig. 2 Cross section of the SWEC chamber [4].

This paper describes the hydrodynamic as well as the thermodynamic states of the SWEC device when interacting with regular waves. Research based on the marine vehicles with trapped air cavities [6] was used along with linear wave theory, Newton's second law and the ideal gas law to derive the constitutive equations that describe the various states in the system. These equations allow for the cavity's free-surface elevation and pressure oscillation to be modelled. In addition, the auxiliary volume pressure, the systems mass flow rate and the conversion efficiency are also calculated.

Scale model experiments were carried out in a wave flume to verify the simulation model. A 1:25 scale model based on Froude scaling was tested in a wave flume of the Civil Engineering Department at Stellenbosch University. The wave flume is 28m long and can generate a range of regular waves. This allowed the scale model to be tested not only in the design conditions but as well as conditions which varied from the design conditions.

II. MATHEMATICAL MODEL

This section describes the development of the simulation model and the physical systems, which it represents.

The mathematical model used to describe this system is similar to the one derived in [6] and the detailed derivation and adaptation of this model can be found in [2], the most influential changes include those made to the expressions used to model the orifice power take-off and the added mass phenomena. The model makes use of linear wave theory in conjunction with work done on air cavities trapped in marine vehicles [7].

Various assumptions were made for the modelling process. Firstly, the waves passing over the device are assumed to be unaffected by the presence of the structure. This means that no wave scattering or wave radiation was considered. In the real world, this is not the case as when energy is extracted from the waves it will have an effect on the waves passing overhead. Secondly, the water column is assumed as a solid vertical mass with a flat-water surface as seen in Fig. 3. The temperature of the system is assumed to stay constant (isentropic) as the pressure and volume changes are very small. Finally, the turbulence which will be present in the water column as well as the air chamber and outlet duct is not modelled, but is instead included as losses when dealing with the mass flow rate in the system. See Fig. 3 for a schematic of the physical system.

1) *Hydrodynamic state equation:* The first part of the system to be modelled is the movement of the water column inside the chamber and the corresponding water level height, *z(t)*. Newton's second law is applied to this volume of water that results in the following equation,

$$M\ddot{z} + B\dot{z} + Cz = F(t) \tag{1}$$

Where M is the mass of the water column, B is the damping coefficient and C is the hydrostatic restoring force. The damping coefficient is assumed as a function of the mass, M as well as the added mass, M_a. The expression which defines the added mass associated with this system is found in [8]. The hydrostatic restoring coefficient is assumed to be 10% of the critical restoring coefficient value. This value was found to be a suitable approximate by [9] who carried out theoretical and experimental investigations on trapped and submerged bodies of air.

The total force acting on the bottom of the water column is made up of three forces. Firstly the added mass force $F_a(t)$ which is a damping force. Secondly the Froude-Krylov force $F_{FK}(t)$ which is present at the bottom of the water column and thirdly the force due to varying air pressure in the chamber $F_{\Delta Pair}(t)$ (the forces can been seen in Fig. 3). This results in,

$$F(t) = F_a(t) + F_{FK}(t) + F_{\Delta Pair}(t) \tag{2}$$

Making use of linear wave theory and various mathematical manipulations, expressions for the various forces are developed. The parameters α and β are introduced in order to simply the equation of motion,

$$\alpha = d_2 + \frac{M_a}{(a' b')} \tag{3}$$

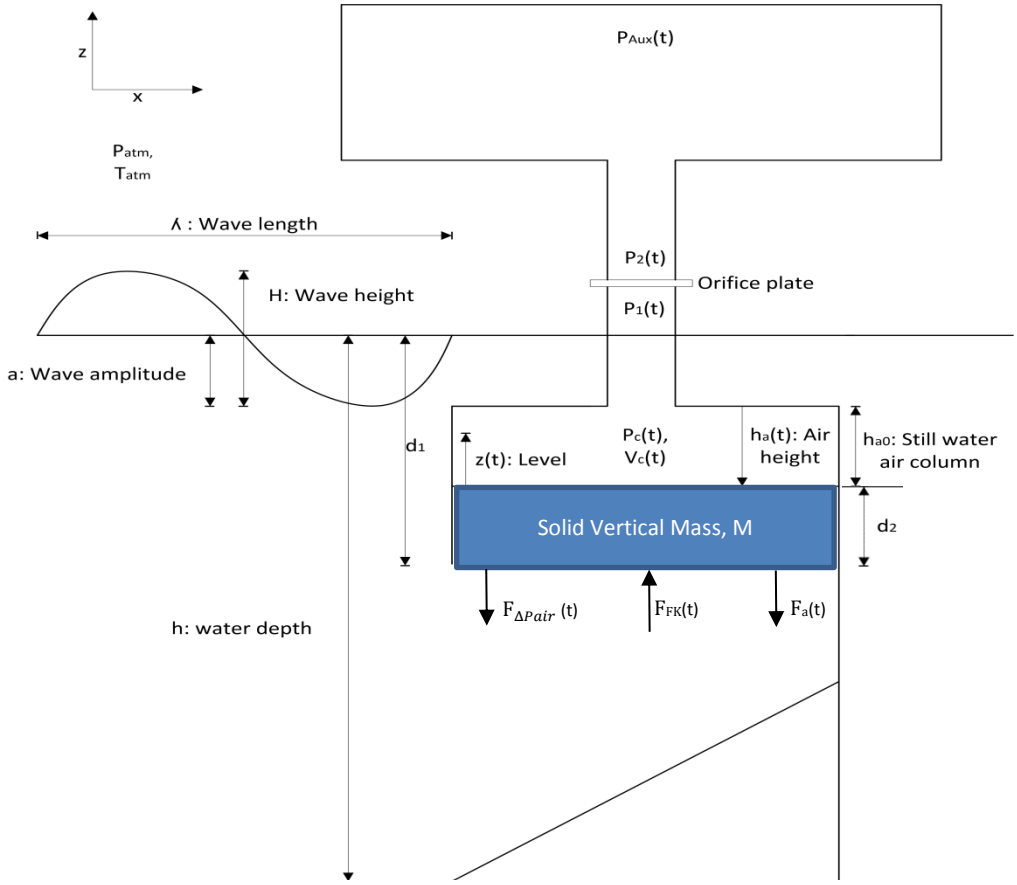

Fig. 3 Schematic of the SWEC experimental setup.

$$\beta = \frac{gcoshk(k(h-d_1))}{cosh(kh)} - \frac{M_a}{(a'\,b')\rho}\omega^2\frac{sinh(k(h-d_1))}{sinh(kh)} \tag{4}$$

Symbols in equation 4 include, a' and b' the length and breadth of the chamber respectively, g the gravitational constant, k the wave number, ρ the density of sea water, ω is angular frequency and h, d_1 and d_2 are shown on Fig 3.

Substituting α and β into the motion of equation results in a simplified state equation for the cavity's inner surface level of the form,

$$\ddot{z} = -0.2\sqrt{\frac{g}{(\alpha+z)}}\dot{z} - \frac{gz}{(\alpha+z)} + \frac{\beta a\cdot cos(\omega t+\phi)}{(\alpha+z)} - \frac{\Delta P(t)}{\rho(\alpha+z)} \tag{5}$$

2) *Thermodynamic state equation:* This section describes the governing equations used to model the pressure of the air inside the chamber and follows the same procedure presented in [6]. The required state equation is derived by using the ideal gas equation,

$$P_c(t)V_c(t) = m_c(t)R^*T_c(t) \tag{6}$$

Where $P_c(t)$ is the pressure inside the chamber, $V_c(t)$ is the volume of the chamber and $m_c(t)$ is the mass of air inside the chamber. R^* is the specific gas constant for air and $T_c(t)$ is the temperature of the chamber. The compression and decompression process of the air trapped inside the chamber is considered to be an isentropic process. This means the process is assumed to be adiabatic and reversible. This assumption allows for the following expression to hold true,

$$P_c(t)V_c(t)^\gamma = constant \tag{7}$$

The head loss equation for flow inside a pipe along with the energy equation for pipe flow is used to define an equation which describes the mass flow rate in the system [10], see Equation 8. ΔP is the difference in pressure between the two chambers and the terms under the divide line in equation 8 represent the loss coefficients in the system.

$$\dot{m}_c(t) = \sqrt{\frac{2\rho_{air}|\Delta P(t)|}{\frac{k_f}{a_f{}^2}+\frac{k_{ec1}}{a_{ec1}{}^2}+\frac{k_{ec2}}{a_{ec2}{}^2}+\frac{k_{op}}{a_{op}{}^2}}} \times sign\big(\Delta P(t)\big) \tag{8}$$

Equations 6, 7 and 8 are used to derived the final state equation for the pressure in the chamber,

$$\dot{P}_c(t) = -\frac{{C_s}^2 C_d}{\left(a' b'\right)(h_{a0} - z)}\sqrt{2\rho_{air}|P_c(t) - P_{aux}(t)|} + \gamma \frac{P_c(t)}{h_{a0} - z}\dot{z} \quad (9)$$

Where C_s is the speed of sound through air and is substituted for $\gamma R^* T_c$, C_d is the coefficient of discharge which incorporates losses from the orifice plate as well as friction and expansion and contraction losses, ρ_{air} is the average density of the air in the system and $P_{aux}(t)$ is the pressure in the auxiliary volume seen in Equation 10.

$$P_{aux}(t) = P_{atm} + \rho_w g(d_1 - d_2) + \frac{\Delta m_{aux}(t) R^* T_{aux}}{V_{aux}} \quad (10)$$

The results produced by this model are compared with experimental results in Section IV.

III. Experimental Model

This section describes the experimental setup which was used to test the scale model of the SWEC. The experimental model was constructed using the original SWEC chamber dimensions [5] at a scale of 25:1 as well as certain design adaptations suggested by [11]. These design adaptations included the positioning of the orifice flowmeter, the diameter of the orifice flow metre and the size of the auxiliary chamber.

A. Instrumentation and setup

In order to calculate the wave power converted by the SWEC into pneumatic power, the volumetric flow rate in the system as well as the pressure difference between the cavity and the auxiliary volume were required. As Equation 11 shows, the converted power is defined as the product of volumetric flow rate and the pressure difference [12]. The power take-off mechanism for this system is an orifice flow plate. The orifice plate is also used to determine the volumetric flow rate in the system. This is done by using a known relationship between the pressure drop over the orifice plate and the volumetric flow rate.

$$P_{converted}(t) = V(t) \times \Delta P(t) \quad (11)$$

Differential pressure transducers were used to measure the pressure drop over the orifice plate and the differential pressure between the cavity and the auxiliary volume. Another important measured parameter is the water height inside the cavity, this was recorded using a wave probe. In order to determine the efficiency of the device the input wave power was required and thus a wave probe was used to measure the exact input wave height and period at the chambers opening. An extra wave probe was situated a few metres after the device in order to measure the total wave power absorbed by the device. A thermometer was placed next to the wave flume and temperatures were recorded every 3 hours. See Fig. 4 for a photo of the setup.

B. Calibration

The differential pressure transducers were calibrated using an extremely accurate Betz manometer. The orifice flow plate meter was calibrated by recording the pressure drop over the plates whilst running a known volumetric flowrate through the system using a *Disa* calibration unit. The wave probes were calibrated daily by using a *HP Wallingford* DAQ (Data Acquisition).

C. Experiments

The SWEC setup was tested with 5 different orifice plates, for 8 different wave periods and 3 different wave heights. The three plates which proved to be most efficient in orientation 1 were tested in orientation 2. The plate which proved to be the most efficient in orientations 1 and 2 was tested in orientations 3, 4 and 5. See Fig. 5 for the various orientations.

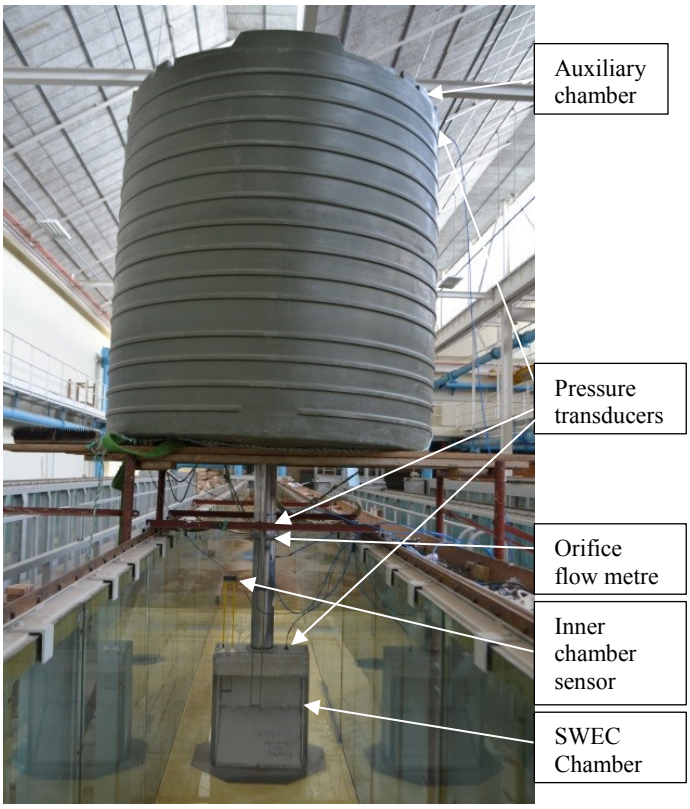

Fig. 4 Photo of the SWEC setup.

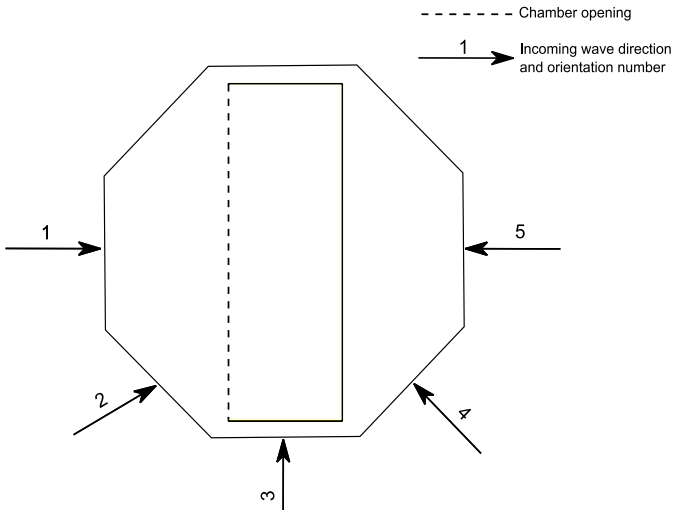

Fig. 5 Different orientations of the incident waves.

IV. Experimental Results

In this section the experimental results are compared with the results produced by the mathematical model. It must be stated that when referring to waves produced at certain heights there is a deviation between the intended wave height and actual wave height. This is due to the fact that there will always be reflection and refraction present in a wave flume causing the desired input waves to differ from the actual input waves. An average deviation of less than 5.5% was achieved for the experimental testing. The graphed results make use of dimensionless numbers to compensate for this deviation. The test facility wave maker was equipped with active absorption and a 20-metre beach with porous breakwaters and absorption foam was used to dissipate the waves that passed the test structure.

The orifice plates are named by percentages, 0.25%, 0.5% and 1%. These percentage represent the ratio of the area of the orifice hole to the area of the free water surface inside the chamber. Meaning that the 0.25% plate has the smallest diameter hole and the 1% plate has the largest hole. The two most important results are presented in this paper, the conversion efficiency and transmissibility. The conversion efficiency refers to the ratio of average converted power to available power in the wave, $\frac{P_{converted}}{P_{wave}}$. The transmissibility refers to the ratio of the inner chamber amplitude (the amplitude of the waterline inside the chamber) to the input wave amplitude and therefore the 'transmissibility of water into the chamber'. These results were defined as the most useful results for confirming the models accuracy and for making conclusions on the viability of the device as a WEC.

See Fig. 6 for the measured and simulated conversion efficiency in orientation 1 at a wave height of 0.09 m for various wave periods. After analysing the predicted conversion efficiencies, the overall average error percentage between predicted and measured results for all tests carried out proved to be 12%. Fig. 7 shows the transmissibility of the SWEC, the overall average error percentage between predicted and measured transmissibility results for all tests carried out proved to be 5%. It is expected that the transmissibility of the system would be predicted more accurately as it is less complex than the predicting the power conversion. The power conversion involves losses throughout the airflow system that transmissibility predictions do not need to account for.

Fig. 8 shows the efficiency of the SWEC in the 5 different orientations shown in Fig. 5. Fig. 8 shows a general decrease in efficiency with an increase in period, the overall maximum efficiency being 18% at a period of 1.75 s and 13% at the expected operating conditions. The SWEC was designed to operate at a 60° angle with regards to the incoming wave, this is supported by the fact that orientation 2 (at 45°) proved to be the most efficient orientation.

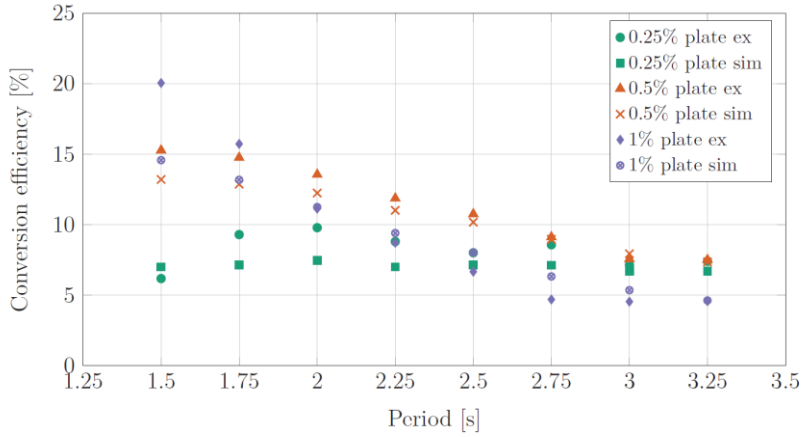

Fig. 6 Measured and simulated conversion efficiency in orientation 1 at a wave height of 0.09 m for various wave periods.

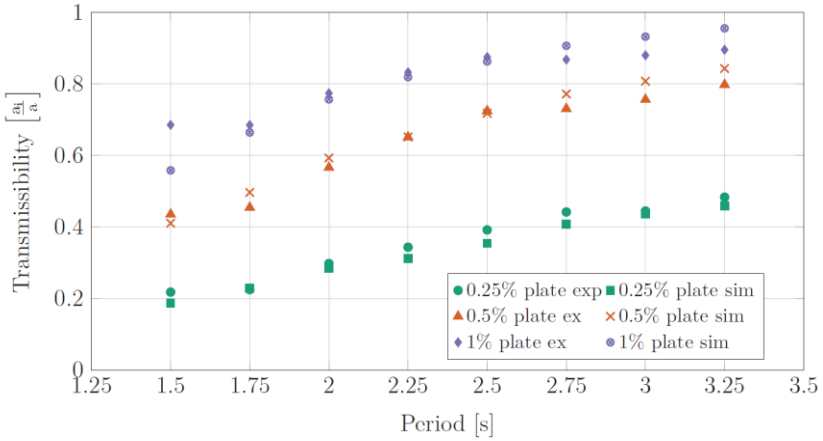

Fig. 7 Measured and simulated transmissibility in orientation 1 at a wave height of 0.09 m for various wave periods.

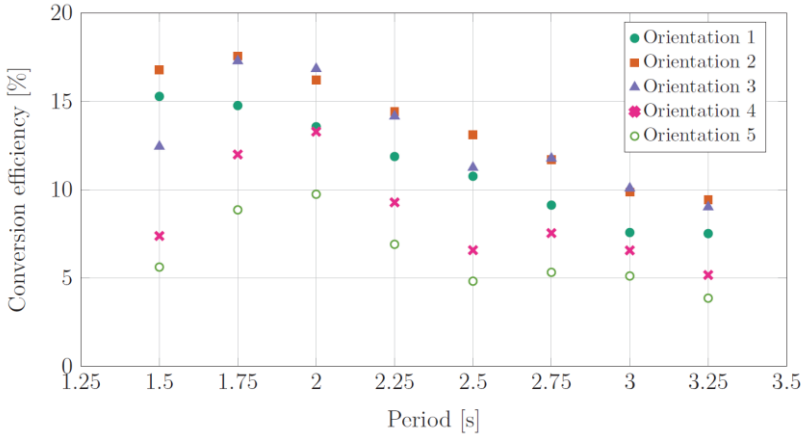

Fig. 8 Measured conversion efficiency in various orientations at a wave height of 0.09 m for various wave periods using the 0.5% plate.

V. Full-Scale Model Application

The simulation model was run using input data sourced from a wave buoy off the south east coast of South Africa near the port of East London [13]. The data was gathered by a directional Datawell Waverider buoy, situated at 33°2'16.80"S, 27°55'50.99"E in a water depth of 27 m, about 1.2 km off the tip of the breakwater. Measurements were processed on board, and transmitted to a shore station every half-hour. The analysed data was then downloaded in near real-time to the Stellenbosch office of the CSIR, where it is stored in a database. See Fig. 9 for the geographical position of the wave buoy.

The data was captured and processed into three-hourly averages and includes significant wave height, wave period, wave direction, average spread and maximum wave height. The data set ranges from the year 2009 to the year 2016; the year 2010 was omitted for this study as the data set for that year was incomplete due to unplanned maintenance on the buoy.

Fig. 10 shows the average wave power per metre wave front recorded by the buoy from 2007 to 2016. The annual trends do not repeat themselves but there is an overall visible increase in power available during the winter months.

Fig. 9 East London harbour and the position of the wave buoy (33° 2'16.80"S, 27°55'50.99"E).

This data was used to produce frequency tables that convey the percentage of time during which a certain wave condition occurred. See Table III for the number of times a certain wave condition was present for a three-hour averaged period in 2016.

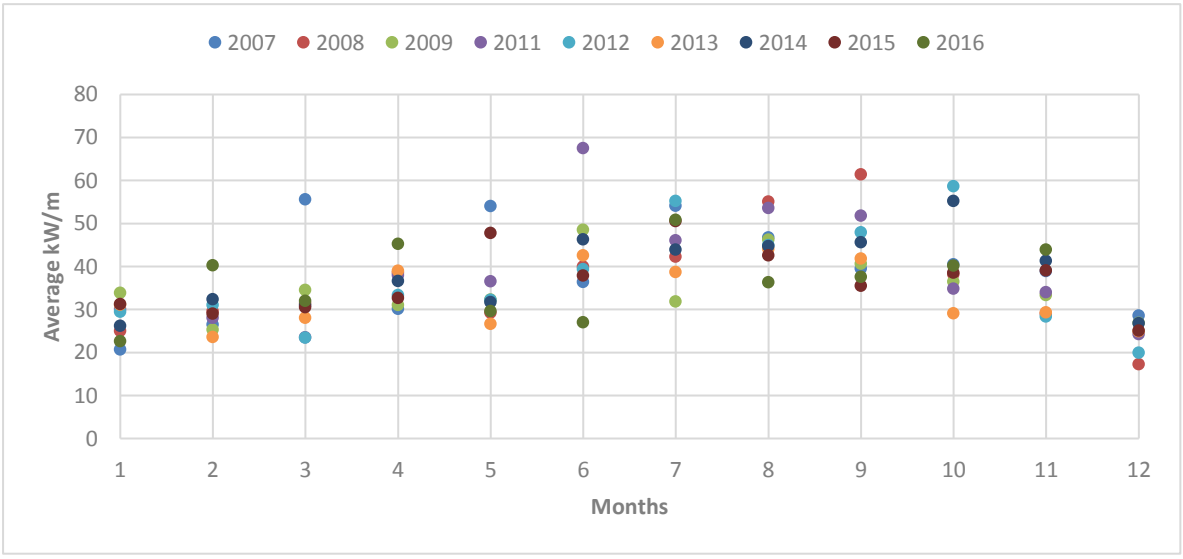

Fig. 10 Average wave power per metre wave front recorded by the East London Datawell Waverider buoy [13].

TABLE IV
NUMBER OF THREE-HOUR OCCURRENCES OF CERTAIN CONDITIONS IN 2016.

Tp(s) \ Hm0 (m)	0.5-1	1-1.5	1.5-2	2-2.5	2.5-3	3-3.5	3.5-4
3-6	0	5	13	4	0	0	0
6-9	0	63	77	41	10	0	1
9-12	44	508	449	260	68	19	6
12-15	11	201	322	180	63	27	7
15-18	0	36	67	55	20	14	7
18-21	0	6	2	3	0	0	0

A MATLAB script file was used to generate a typical sea-state associated with the wave height and period parameters specified by the measured data. The JONSWAP spectrum was used to generate these sea-states, as it is one of the more accurate representations of full-scale sea-states. The generated sea-states were scaled down and used as input into the simulation model. The model output predicts the power output for a single chamber. To predict the output of a full-scale model, the output was scaled back up and multiplied by the number of chambers in a full-scale SWEC. The assumption is made that the chambers will all produce the same amount of power when in the same wave conditions. Due to low directional variation of the wave data (11% average deviation from the mean) the SWEC is assumed to be hit head on by the waves.

The full-scale power results for a single chamber are displayed in Table V. This Table shows how the chamber reacts in different sea-states, ideally the chamber should be 'tuned' to be most efficient when operating in the most frequently found wave conditions. Tables II and Table III show that there is a mismatch between the higher levels of energy production and the sea-state frequency at the selected site.

TABLE VII
PREDICTED AVERAGE KW PRODUCED PER CHAMBER FOR VARIOUS SEA-STATES IN 2016.

Tp(s) \ Hm0 (m)	0.5-1	1-1.5	1.5-2	2-2.5	2.5-3	3-3.5	3.5-4
3-6	2	2	5	7	10	13	17
6-9	4	11	21	34	48	59	82
9-12	5	15	26	42	63	84	102
12-15	4	12	23	45	60	81	101
15-18	2	9	19	27	58	63	80
18-21	2	7	14	23	46	59	73

The average power ratings were multiplied by the corresponding periods during which the specific wave conditions occurred, this results in a table showing the predicted energy produced by a single full-scale chamber for 2016. See Table IV for the annual energy spread over wave height and period. It must be stated that this is mechanical energy available after the turbine process, losses in the electrical generation and transmission will still be present before the electrical energy can be used.

After analysing Tables III and VII and carrying out high-level optimisation, a plant size (made up of 24 chambers, two sets of 12 in each arm) of 1.56 MW was defined. Summing the predicted energy produced over the year of 2016 and assuming a 10% loss over the generator and transmission lines leads to a total annual generation of 4 289 MWh of electrical energy per SWEC plant and a capacity factor calculated as 35%.

TABLE VIII
PREDICTED MWH PRODUCED PER CHAMBER FOR 2016 (VARIABLE TURBINE SIZE).

Tp(s) \ Hm0 (m)	0.5-1	1-1.5	1.5-2	2-2.5	2.5-3	3-3.5	3.5-4
3-6	0	0	0	0	0	0	0
6-9	0	2	5	4	1	0	0
9-12	1	23	35	33	13	5	2
12-15	0	7	22	24	11	7	2
15-18	0	1	4	5	3	3	2
18-21	0	0	0	0	0	0	0

VI. CONCLUSIONS

A. *Mathematical model verification*

The mathematical model derived for the SWEC exhibited the ability to predict converted power with relatively high accuracy (overall average error of 12%). The accuracy proved to be higher for input waves with lower frequencies and less accurate for input waves with higher frequencies. The simulation model predicted the inner surface level with a higher accuracy with an overall average error of 5%. Deviation between the simulated results and experimental results were due to aspects such as diffraction and turbulences that were not modelled but rather assumed as a loss. The model derived in this paper could still be further adapted in order to increase the accuracy and ability to model the actual behaviour of the system. The current model proved to be useful in the predicting the output of the SWEC in full-scale irregular wave conditions.

B. *SWEC as a viable WEC*

The conversion efficiency of 13% at operating conditions does not fully support the implementation of the device as a WEC. The results shed light on the conditions in which the device would optimally operate and suggest that the SWEC has the potential to be a viable WEC if effective optimisation were to be carried out.

The analysis carried out using full-scale sea-states estimates an average annual production of 4 289 MWh per SWEC plant with a capacity factor of 35%. Comparing this to South Africa's largest wind energy plant which averages around 460 000 MWh of annual energy output with a capacity factor of 38%, makes the SWEC plant competitive in terms of capacity factor. This being said, the inherent complexities involved with deployment and operation of a device beneath the ocean's surface will make it extremely difficult for the SWEC to be economically competitive. In order to compare the SWEC technology with current renewable energy technologies, the levelised cost of energy (LCOE) needs to be investigated. It is expected that at conversion efficiencies lower

than that of today's solar photovoltaic modules (13% predicted by this study), the cost of converting energy under the sea would be too great. If the SWEC design were to improve its conversion efficiency and take full advantage of the high energy density present in the ocean, the LCOE could become competitive.

A positive of wave energy exhibited by this study is its consistency. Table II shows that the wave conditions at the recording site were between 1 and 2.5 metres high with a period of between 9 and 15 seconds for 74% of the time in 2016. The data for the years 2006 to 2015 also agree with this, demonstrating the consistent nature of wave energy.

The deeper a WEC's is placed in the ocean the better its survivability but the lower its conversion efficiency. The results produced by this study support this observation and provide an opportunity for a study on the optimal depth and configuration of a SWEC. Another interesting aspect of OWC WEC's is the contribution of both the wave's kinetic energy and potential energy to converted energy. The experiments conducted on the SWEC chamber in various positions present an opportunity to further investigate this phenomenon.

ACKNOWLEDGMENTS

Thanks are due to the Stellenbosch University Mechanical and Civil Engineering labs and staff, as without their help and equipment this project would not have been possible.

REFERENCES

[1] J. R. Joubert, "An investigation of the wave energy resource on the South African cost, focusing on the spatial distribution of the south west coast," M. Eng. thesis, Stellenbosch University, Stellenbosch, South Africa, Nov. 2008.

[2] J. Fairhurst, "Modelling and Design of an Oscillating Wave Energy Converter," M. Eng. thesis, Stellenbosch University, Stellenbosch, South Africa, November. 2015.

[3] J. Fairhurst, J.L. Van Niekerk, "Modelling, simulation and testing of a submerged oscillating water column," International Journal of Marine Energy, vol. 16, pp. 181-195, December. 2016.

[4] G de F. Retief, G.K. Muller, F. P. J. Guestyn, and D.H. Swart, "Detailed design of a wave energy conversion plant," *ICCE.*, vol. 21, pp. 2546–2562, June. 1982.

[5] P. H.Ackerman, "Air Turbine Study for a Wave Energy Conversion System," M. Eng. thesis, Stellenbosch University, Stellenbosch, South Africa, October. 2009.

[6] R. Gervelas, F. Trarieuxand, M. Patel, "A time-domain simulator for an oscillating water column in irregular waves at model scale," *Ocean Engineering.*, vol. 38, pp. 1007-1013, September. 2010.

[7] M. H. Patel, "Hydrostatic analysis of marine vehicles with trapped air cavities," *International Shipbuilding Progress.*, vol. 34, pp. 64-74, 1978.

[8] R. G. Dong, "Effective mass and damping of submerged structures,",Research report, University of California, Livermore, California, U.S.A,April. 1978.

[9] M.H. Patel, J.H.Harrison, "The mechanics of a compliant motion suppression system for semisubmersibles model scale," *Sound and Vibration.* vol. 106, pp. 491-507, July. 1985.

[10] M. W.Holtz, "Modelling and Design of a Novel Air-Spring for a Suspension Seat,", M. Eng. thesis, Stellenbosch University, Stellenbosch, South Africa, December. 2007.

[11] N. Dizadji, S. E. Sajadia, "Modelling and optimization of the chamber of OWC system," *Energy.*, vol. 36, pp. 2360–2366, January. 2011.

[12] Y. Zhang, Q. P. Zhu, D. Greaves, "Air-water two-phase flow, modeling the hydrodynamic performance of an oscillating water column device," Renewable Energy., vol. 41, pp. 159–170, October. 2012.

[13] (2017) CSIR. [Online]. Available: http://wavenet.csir.co.za/OnlineData/EastLondon/eastlondon.htm